RESEARCH ARTICLE

Application of chemokine receptor antagonist with stents reduces local inflammation and suppresses cancer growth

Ai-Wu Mao[1,2] · Ting-Hui Jiang[1,2] · Xian-Jun Sun[2] · Jian Peng[1]

Abstract Severe pain and obstructive jaundice resulting from invasive cholangiocarcinoma or pancreatic carcinoma can be alleviated by implantation of biliary and duodenal stents. However, stents may cause local inflammation to have an adverse effect on the patients' condition and survival. So far, no efficient approaches have been applied to prevent the occurrence of stents-related inflammation. Here, we reported significantly higher levels of serum stromal cell-derived factor 1 (SDF-1) in the patients that developed stents-associated inflammation. A higher number of inflammatory cells have been detected in the cancer close to stent in the patients with high serum SDF-1. Since chemokine plays a pivotal role in the development of inflammation, we implanted an Alzet osmotic pump with the stents to gradually release AMD3100, a specific inhibitor binding of SDF-1 and its receptor C-X-C chemokine receptor 4 (CXCR4), at the site of stents in mice that had developed pancreatic cancer. We found that AMD3100 significantly reduced local inflammation and significantly inhibited cancer cell growth, resulting in improved survival of the mice that bore cancer. Moreover, the suppression of cancer growth may be conducted through modulation of CyclinD1, p21, and p27 in the cancer cells. Together, these data suggest that inhibition of chemokine signaling at the site of stents may substantially improve survival through suppression of stent-related inflammation and tumor growth.

Introduction

Pancreatic adenocarcinoma frequently results in malignant obstruction of the common bile duct (CBD) and digestive tract [1–4]. When the pancreatic adenocarcinoma are not resectable, palliative management of biliary and duodenal stenoses is believed to enhance the quality of life of patients by reducing pruritus, ascending cholangitis, vomiting, and cachexia [1–4]. Transhepatic biliary stenting and self-expandable metallic enteral stents have a well-established efficacy in the palliative management of malignant biliary stenosis [5–7]. However, although severe pain and obstructive jaundice resulting from invasive cholangiocarcinoma or pancreatic carcinoma can be alleviated by implantation of biliary and duodenal stents, the implanted stents may cause local inflammation to have an adverse effect on the patients' condition and survival [5–10]. So far, no efficient approaches have been applied to prevent the occurrence of stents-related inflammation.

The stromal cell-derived factor 1 (SDF-1) is also known as C-X-C motif chemokine 12 (CXCL12), which is an important member of the chemokine family that activate leukocytes to initiate inflammatory processes [11–13]. SDF-1 is potently chemotactic for lymphocytes and macrophages. SDF-1 recruits inflammatory cells through a C-X-C chemokine receptor 4 (CXCR4)-dependent manner [11–13]. Recently, SDF-1/CXCR4 axis has been described as a retention signal for M2 macrophages [13, 14]. Nevertheless, a role of SDF-1 in the development of stents-associated inflammation has not been acknowledged.

✉ Jian Peng
   aiwu_mao@163.com; pengjian1698@aliyun.com

1   Xiangya Hospital of Central South University, 87 Xiangya Road, Changsha 410008, China

2   Interventional Center, St. Luke's Hospital of Jiaotong University School of Medicine, 786 Yuyuan Road, Shanghai 200050, China

Here, we reported significantly higher levels of serum SDF-1 in the patients that developed stents-associated inflammation. A higher number of inflammatory cells have been detected in the cancer close to stent in the patients with high serum SDF-1. Since chemokine plays a pivotal role in the development of inflammation, we implanted an Alzet osmotic pump with the stents to gradually release AMD3100 [14], a specific inhibitor binding of SDF-1 and its receptor CXCR4, at the site of stents in mice that had developed pancreatic cancer. We found that AMD3100 significantly reduced local inflammation and significantly inhibited cancer cell growth, resulting in improved survival of the mice that bore cancer. Moreover, the suppression of cancer growth may be conducted through modulation of CyclinD1, p21, and p27 in the cancer cells. Together, these data suggest that inhibition of chemokine signaling at the site of stents may substantially improve survival through suppression of stent-related inflammation and tumor growth.

Materials and methods

Patient samples

Eighty-seven paired patients with pancreatic cancer who had received stents treatment were involved in the current study. All the patients had been diagnosed at Interventional Center, St. Luke's Hospital of Jiaotong University School of Medicine from 2007 to 2013. For the use of these clinical materials for research purposes, prior patient's consents and approval from the Institutional Research Ethics Committee were obtained.

Pancreatic cancer cells

Human pancreatic cancer cell line (PANC-1) has been generated from a human carcinoma of the exocrine pancreas in 1975 [15] and was purchased from the American Type Culture Collection (ATCC; Rockville, MD, USA). PANC-1 was cultured in Dulbecco's Modified Eagle's Medium (DMEM) supplemented with 20 % fetal bovine serum (Invitrogen, Carlsbad, CA, USA). To trace PANC-1 in vivo, they were transduced with an adeno-associated virus (AAV) carrying a luciferase and a green fluorescent protein (GFP) reporter (AAV-luc), as has been previously described [16–18]. The transduced cells were purified based on GFP by flow cytometry.

Animal handling

All mouse experiments were approved by the Animal Research and Care Committee at the Interventional Center of St. Luke's Hospital of Jiaotong University School of Medicine. Nonobese diabetic/severe combined

immunodeficiency (NOD/SCID) mice were purchased from the Jackson Labs (Bar Harbor, ME, USA). Only 12-week-old male NOD/SCID mice were used in the current study.

Luciferase-carrying PANC-1 cells (PANC-1-Luc, 10^6) were directly injected into the parenchyma of the pancreas in NOD/SCID mice, as has been described before [14]. Twelve weeks after cancer cell implantation, tumor development was confirmed and quantified by bioluminescence detection, using IVIS Imaging System (Xenogen Corp., Alameda, CA, USA). To inhibit SDF-1/CXCR4 interaction, 2 mg AMD3100 (Sigma-Aldrich, St. Louis, MO, USA) was dissolved in phosphate-buffered solution (PBS) and placed in mini-osmotic pumps (Alzet Osmotic Pumps, Cupertino, CA, USA), which were implanted subcutaneously to the mice, at the time of stent placement which requires handling with a dissection microscope as has been described before [19]. Mini-pumps containing saline were implanted in control mice. After another 4 weeks, bioluminescence was measured again. For bioluminescence quantification, all of the images were taken 10 min after intraperitoneal injection of luciferin (Sigma-Aldrich) of 150 mg/kg body weight, as a 60-s acquisition and 10 of binning. During image acquisition, mice were sedated continuously via inhalation of 3 % isoflurane. Image analysis and bioluminescent quantification were performed using Living Image software (Xenogen Corp). Ten mice were analyzed in each group.

Immunohistochemistry (IHC) and quantification

The human specimen or mouse samples were fixed in 4 % formalin for 6 h, followed by cryo-protection in 30 % sucrose overnight, and then sectioned at 6 μm. IHC was then performed, followed by counterstaining with hematoxylin. The primary antibodies are polyclonal rat anti-F4/80 (Invitrogen, St. Louis, MO, USA) and rat anti-Ki-67 (DAKO, Carpinteria, CA, USA). For quantification, 5 random fields were quantified in each slides, and in each animals; at least 5 slides that were 100 μM away from each other were counted. Quantification was done in 10 mice in each condition.

ELISA

The concentration of serum SDF-1 and tissue IL-6, tumor necrosis factor alpha (TNF-α), and interferon-gamma (IFN-) was determined by ELISA Kit (R&D Systems, Los Angeles, CA, USA). ELISA was performed according to the instructions of the manufacturer. Briefly, the extracted protein was added to a well coated with primary antibody and then immunosorbented by biotinylated primary antibody at room temperature for 2 h. The color development catalyzed by horseradish peroxidase was terminated with 2.5 mol/l sulfuric acid, and the absorption was measured at 450 nm. The protein

concentration was determined by comparing the relative absorbance of the samples with the standards.

Western blot

Protein was extracted from the tissue with RIPA lysis buffer (1 % NP40, 0.1 % sodium dodecyl sulfate (SDS), 100 μg/ml phenylmethylsulfonyl fluoride, 0.5 % sodium deoxycholate, in PBS) on ice. The supernatants were collected after centrifugation at $12,000 \times g$ at 4 °C for 20 min. Protein concentration was determined using a BCA protein assay kit (Bio-rad, China), and whole lysates were mixed with 4× SDS loading buffer (125 mmol/l Tris–HCl, 4 % SDS, 20 % glycerol, 100 mmol/l dithiothreitol (DTT), and 0.2 % bromophenol blue) at a ratio of 1:3. Samples were heated at 100 °C for 5 min and were separated on SDS-polyacrylamide gels. The separated proteins were then transferred to a PVDF membrane. The membrane blots were first probed with a primary antibody. After incubation with horseradish peroxidase-conjugated second antibody, autoradiograms were prepared using the enhanced chemiluminescent system to visualize the protein antigen. The signals were recorded using X-ray film. Primary antibodies were rabbit anti-CyclinD1, anti-p21, anti-p27, and anti-α-tubulin (Cell Signaling, San Jose, CA, USA). Secondary antibody is HRP-conjugated anti-rabbit (Jackson ImmunoResearch Laboratories, West Grove, PA, USA). α-Tubulin was used as protein loading controls. The protein levels were first normalized to α-tubulin and then normalized to control.
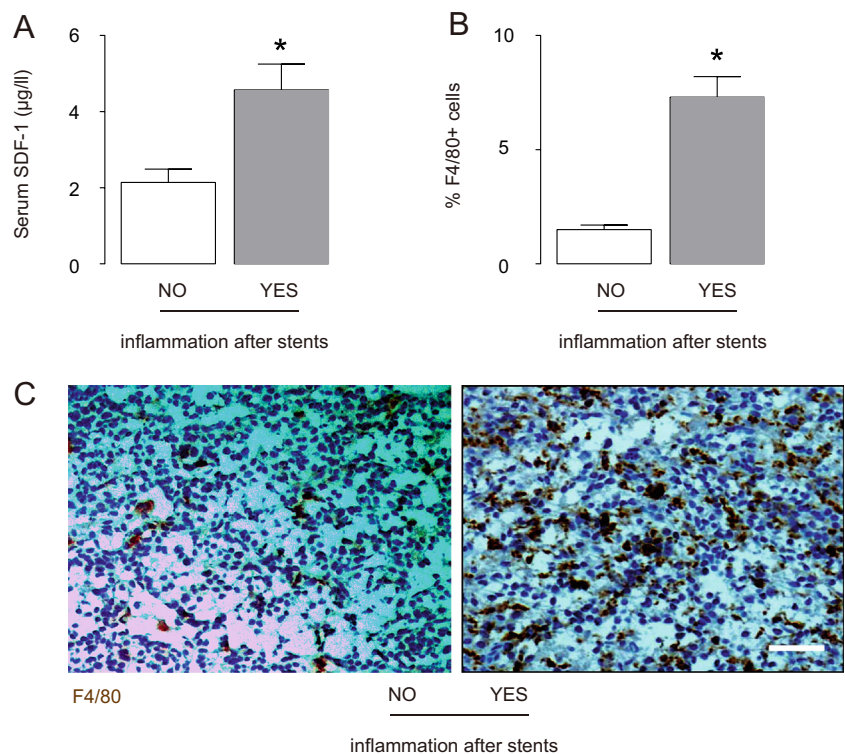
Statistical analysis

All statistical analyses were carried out using the SPSS 17.0 statistical software package. All values are depicted as mean± standard deviation and are considered significant if $p<0.05$. All data were statistically analyzed using one-way ANOVA with a Bonferoni correction and followed by Fisher's exact test to compare two groups.

Results

Serum SDF-1 level is a good maker for stents-associated inflammation

Although implantation of biliary and duodenal stents has been shown to release severe pain and obstructive jaundice resulting from invasive cholangiocarcinoma or pancreatic carcinoma, stents may cause local inflammation to have an adverse effect on the patients' condition and survival. Here, we addressed to this question.

We examined the serum SDF-1 levels in 87 patients with pancreatic cancer who had received stents treatment. We found that 39 patients who had developed stents-associated inflammation had higher levels of serum SDF-1 compared to those 48 who did not develop stents-associated inflammation (Fig. 1a). Thus, SDF-1 appeared to be a good marker for stents-associated inflammation. From the resected cancer specimen close to the implanted stents, we detected a higher
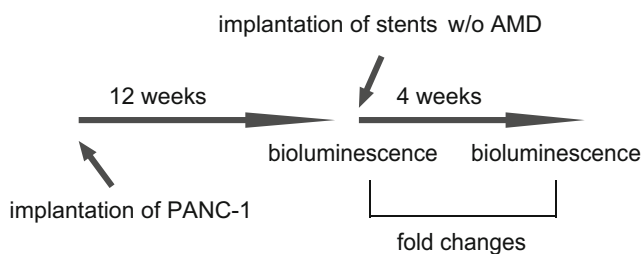
Fig. 1 Serum SDF-1 level is a good maker for stents-associated inflammation. **a** We examined the serum SDF-1 levels in 87 patients with pancreatic cancer who had received stents treatment. We found that 39 patients who had developed stents-associated inflammation had higher levels of serum SDF-1 compared to those 48 who did not develop stents-associated inflammation. **b–c** From the resected cancer specimen close to the implanted stents, we detected a higher number of inflammatory macrophages based on F4/80 staining in the patients with higher serum SDF-1 and stents-associated inflammation, by quantification (**b**) and representative image (**c**). *$p<0.05$. Scale bar is 50 μm

Fig. 2 Experimental model to examine the role of SDF-1 in stents-associated inflammation. A human PDAC cell line, PANC-1, was used in our study. To trace these cells in vivo, we transduced them with an AAV carrying a luciferase and a GFP reporter and purified transduced cells based on GFP by flow cytometry. These cells express luciferase to allow in vivo imaging and quantification. Then, these cells were directly injected into the pancreas of NOD/SCID mice. The establishment of the implanted tumor was confirmed by bioluminescence analyses after 12 weeks. Then, NOD/SCID received implantation of the stents, with an Alzet osmotic pump to gradually release AMD3100 (AMD), a specific inhibitor binding of SDF-1 and its receptor CXCR4, at the site of stents in mice that had developed pancreatic cancer. After another 4 weeks, bioluminescence was measured again and compared to the levels at the time of stents and minipump placement in the same animals

number of inflammatory macrophages based on F4/80 staining in the patients with higher serum SDF-1 and stents-associated inflammation, by quantification (Fig. 1b) and representative image (Fig. 1c). These data suggest that stents may induce releases of chemoattractive factor to induce inflammation.

Experimental model to examine the role of SDF-1 in stents-associated inflammation

Since a higher number of inflammatory cells were detected in the cancer close to stent in the patients with high serum SDF-1 (Fig. 1a–c), and since chemokine plays a pivotal role in the development of inflammation, we inhibited the chemokine receptor signaling to see the effects on stents-associated inflammation.

A human pancreatic ductal adenocarcinoma (PDAC) cell line, PANC-1, was used in our study. To trace these cells in vivo, we transduced them with an AAV carrying a luciferase and a GFP reporter and purified transduced cells based on GFP by flow cytometry. These cells express luciferase to allow in vivo imaging and quantification. Then, these cells were directly injected into the pancreas of NOD/SCID mice. The establishment of the implanted tumor was confirmed by bioluminescence analyses after 12 weeks. Then, NOD/SCID received implantation of the stents, with an Alzet osmotic pump to gradually release AMD3100, a specific inhibitor binding of SDF-1 and its receptor CXCR4, at the site of stents in mice that had developed pancreatic cancer. After another 4 weeks, bioluminescence was measured again and compared to the levels at the time of stents and mini pump placement in the same animals (Fig. 2).

Fig. 3 Inhibition of chemokine receptor signaling inhibits stents-associated inflammation and suppresses cancer growth. **a** The levels of IL-6, TNF-α, and IFN- in the mouse cancer tissue close to stents were examined by ELISA. **b–c** Bioluminescence was examined in mice that received stents and AMD3100 (AMD)/ saline pumps, as shown by quantification (**b**) and representative image (**c**). *p<0.05. N=10
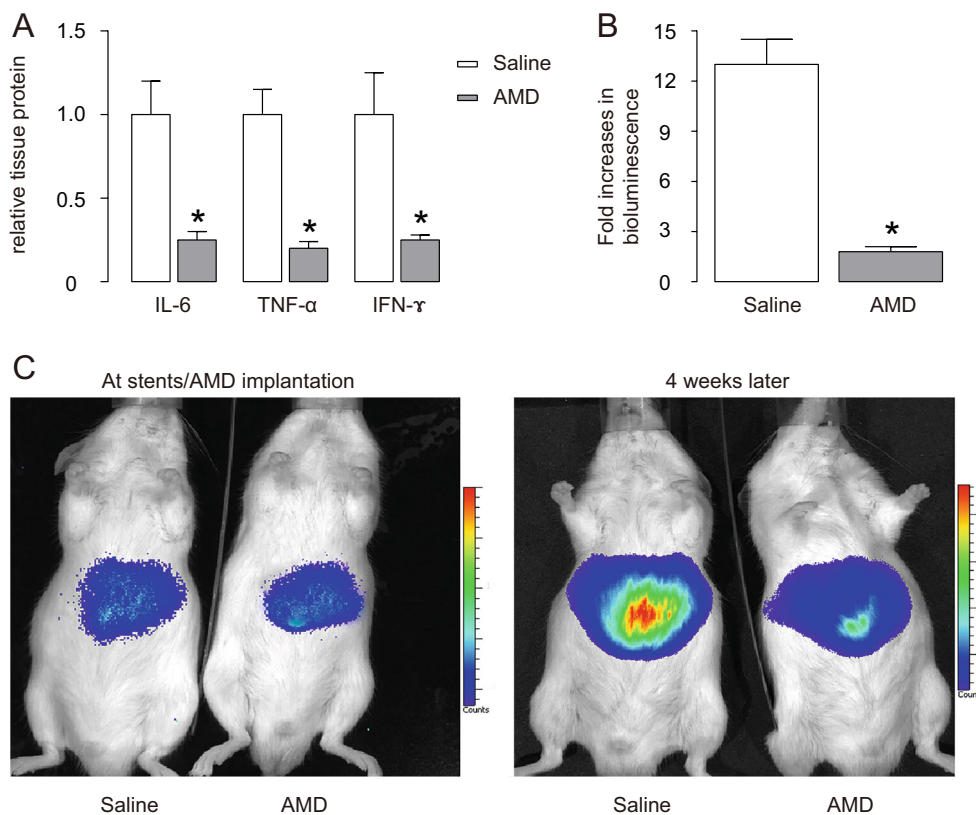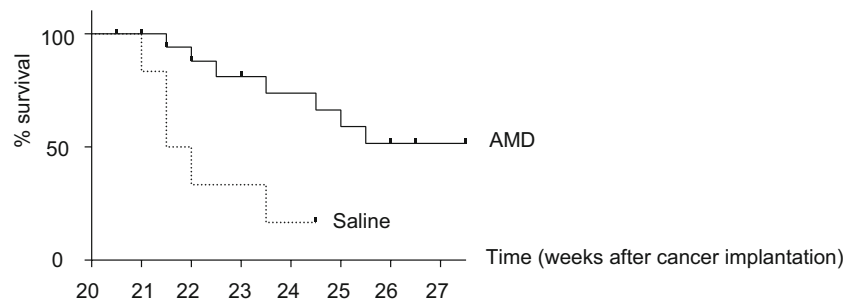
Fig. 4 Inhibition of chemokine receptor signaling improves survival. Kaplan-Meier plot of overall survival in mice that received stents with pumps carrying AMD or saline. $N=10$

Inhibition of chemokine receptor signaling inhibits stents-associated inflammation

We found that AMD3100 significantly reduced local inflammation, manifested by the levels of IL-6, TNF-α, and IFN- (Fig. 3a). These data suggest that inhibition of chemokine receptor signaling inhibited stents-associated inflammation.
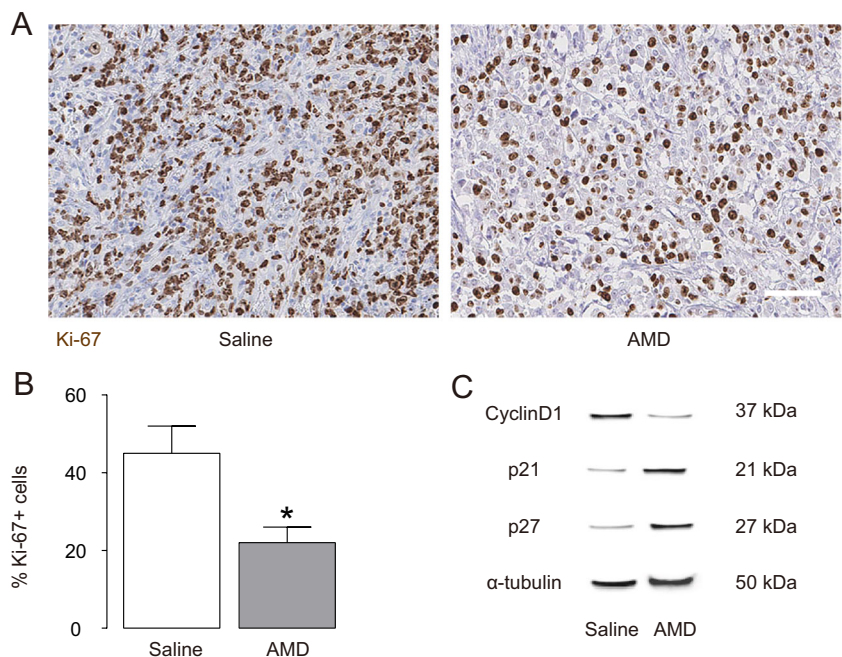
Inhibition of chemokine receptor signaling suppresses cancer growth

Moreover, we found that AMD3100 significantly suppressed cancer cell growth using bioluminescence imaging, as shown by quantification (Fig. 3b) and representative image (Fig. 3c). Moreover, the application of AMD3100 resulted in improved survival of the mice that bore cancer (Fig. 4).

Inhibition of chemokine receptor signaling suppresses cancer growth through modulating CyclinD1, p21, and p27

We examined the underlying mechanisms and found that the suppression of cancer growth by AMD3100 appeared to be resulting from decreased cell proliferation, based on Ki-67 staining (Fig. 5a) and quantification (Fig. 5b). Further, the decreases in cancer cell proliferation could be conducted through modulation of CyclinD1, p21, and p27 in the cancer cells, as shown by representative Western blots (Fig. 5c). Together, these data suggest that inhibition of chemokine signaling at the site of stents may substantially improve survival through suppression of stent-related inflammation and tumor growth, since inflammatory cells have been well-known to release trophic factors to substantialize tumor growth (Fig. 6).

Fig. 5 Inhibition of chemokine receptor signaling suppresses cancer growth through modulating CyclinD1, p21, and p27. **a–b** We examined the underlying mechanisms and found that the suppression of cancer growth by AMD3100 appeared to be resulting from decreased cell proliferation, based on Ki-67 staining (**a**) and quantification (**b**). **c** Western blots for CyclinD1, p21, and p27 in the cancer cells, as shown by representative Western blots. *$p<0.05$. $N=10$
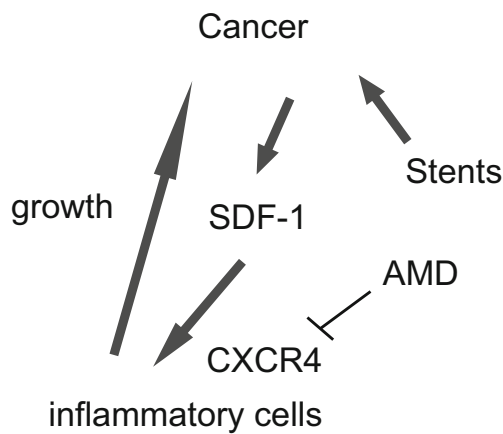
Cancer

Fig. 6 Schematic of the model. Inhibition of chemokine signaling at the site of stents may substantially improve survival through suppression of stent-related inflammation and tumor growth, since inflammatory cells have been well-known to release trophic factors to substantialize tumor growth

Discussion

Pancreatic carcinoma are highly lethal cancers with no cure. Recently, palliative management of biliary and duodenal stenoses is believed to enhance the quality of life of patients who bare unresectable pancreatic carcinoma [1–4]. However, although severe pain and obstructive jaundice resulting from invasive cholangiocarcinoma or pancreatic carcinoma can be alleviated by implantation of biliary and duodenal stents, the implanted stents may cause local inflammation to have an adverse effect on the patients' condition and survival [5–10]. So far, no efficient approaches have been applied to prevent the occurrence of stents-related inflammation. In the current study, we addressed to these questions.

First, we reported significantly higher levels of serum SDF-1 in the patients that developed stents-associated inflammation. A higher number of inflammatory cells have been detected in the cancer close to stent in the patients with high serum SDF-1. Since chemokine plays a pivotal role in the development of inflammation, we implanted an Alzet osmotic pump with the stents to gradually release AMD3100, a specific inhibitor binding of SDF-1 and its receptor CXCR4, at the site of stents in mice that had developed pancreatic cancer. PANC-1 is the most commonly used human PDAC cell line. To trace these cells in vivo, we transduced them with a luciferase reporter, which may allow visualization of the cancer cells in the living animals by provision of the substrate luciferin. These labeled cells were directly injected into the pancreas of immunodeficient NOD/SCID mice, where they could grow without being rejected as mice of normal immunity. AMD3100 was slowly and gradually released in situ so that it could consistently block the binding of the chemoattractive factor SDF-1 to its receptor CXCR4. CXCR4 is expressed by lymphocytes and macrophages. Thus, the recruitment of these

leukocytes to the stents was efficiently blocked, which significantly reduced local inflammation.

Moreover, application of AMD3100 significantly inhibited cancer cell growth, resulting in improved survival of the mice that bore cancer. The suppression of cancer growth may be conducted through modulation of CyclinD1 (a cell-cycle activator), p21, and p27 (two cell-cycle suppressors) in the cancer cells [20–22]. These may result in the prevention of the infiltration of trophic tumor-associated macrophages (TAMs) at the site of cancer, and TAM has been shown to secrete growth factors to promote cell growth in previous studies [23–25]. In the future, effects of co-implantation of AMD3100 with stents on the inflammation and survival in the mouse cholangiocarcinoma and pancreatic carcinoma models should be extensively studied, paying special attention to the cross-talk between carcinoma and tumor-associated macrophages [26–28]. This study may substantially improve our understanding of cholangiocarcinoma and pancreatic carcinoma, as well as the application of stents as a treatment.

Together, our data suggest that inhibition of chemokine signaling at the site of stents may substantially improve subject survival through suppression of stent-related inflammation and tumor growth.

References

1. Srinivasan I, Kahaleh M. Biliary stents in the millennium. Adv Ther. 2011;28:960–72.
2. Deviere J. Pancreatic stents. Gastrointest Endosc Clin N Am. 2011;21:499–510.
3. Gupta R, Reddy DN. Stent selection for both biliary and pancreatic strictures caused by chronic pancreatitis: multiple plastic stents or metallic stents? J Hepatobiliary Pancreat Sci. 2011;18:636–9.
4. Choudhary A, Bechtold ML, Arif M, Szary NM, Puli SR, Othman MO, et al. Pancreatic stents for prophylaxis against post-ERCP pancreatitis: a meta-analysis and systematic review. Gastrointest Endosc. 2011;73:275–82.
5. Thotakura RV, Thotakura S, Sofi A, Bawany MZ, Nawras A. Synchronous EUS-guided choledochoduodenostomy with metallic biliary and duodenal stents placement in a patient with malignant papillary tumor. J Intervent Gastroenterol. 2012;2:88–90.
6. Hamada T, Isayama H, Nakai Y, Togawa O, Kogure H, Kawakubo K, et al. Duodenal invasion is a risk factor for the early dysfunction of biliary metal stents in unresectable pancreatic cancer. Gastrointest Endosc. 2011;74:548–55.
7. Katsinelos P, Kountouras J, Germanidis G, Paroutoglou G, Paikos D, Lazaraki G, et al. Sequential or simultaneous placement of self-expandable metallic stents for palliation of malignant biliary and duodenal obstruction due to unresectable pancreatic head carcinoma. Surg Laparosc Endosc Percutan Tech. 2010;20:410–5.
8. Sica A, Mantovani A. Macrophage plasticity and polarization: in vivo veritas. J Clin Invest. 2012;122:787–95.
9. Shi C, Pamer EG. Monocyte recruitment during infection and inflammation. Nat Rev Immunol. 2011;11:762–74.

10. Wynn TA, Barron L. Macrophages: master regulators of inflammation and fibrosis. Semin Liver Dis. 2010;30:245–57.

11. Tettamanti G, Malagoli D, Benelli R, Albini A, Grimaldi A, Perletti G, et al. Growth factors and chemokines: a comparative functional approach between invertebrates and vertebrates. Curr Med Chem. 2006;13:2737–50.

12. Ruiz de Almodovar C, Luttun A, Carmeliet P. An SDF-1 trap for myeloid cells stimulates angiogenesis. Cell. 2006;124:18–21.

13. Grunewald M, Avraham I, Dor Y, Bachar-Lustig E, Itin A, Jung S, et al. VEGF-induced adult neovascularization: recruitment, retention, and role of accessory cells. Cell. 2006;124:175–89.

14. Cao X, Han ZB, Zhao H, Liu Q. Transplantation of mesenchymal stem cells recruits trophic macrophages to induce pancreatic beta cell regeneration in diabetic mice. Int J Biochem Cell Biol. 2014;53: 372–9.

15. Lieber M, Mazzetta J, Nelson-Rees W, Kaplan M, Todaro G. Establishment of a continuous tumor-cell line (PANC-1) from a human carcinoma of the exocrine pancreas. Int J Cancer. 1975;15: 741–7.

16. Khan IF, Hirata RK, Russell DW. AAV-mediated gene targeting methods for human cells. Nat Protoc. 2011;6:482–501.

17. Grieger JC, Choi VW, Samulski RJ. Production and characterization of adeno-associated viral vectors. Nat Protoc. 2006;1:1412–28.

18. Koerber JT, Maheshri N, Kaspar BK, Schaffer DV. Construction of diverse adeno-associated viral libraries for directed evolution of enhanced gene delivery vehicles. Nat Protoc. 2006;1:701–6.

19. Zhu HD, Guo JH, Mao AW, Lv WF, Ji JS, Wang WH, et al. Conventional stents versus stents loaded with (125)iodine seeds for the treatment of unresectable oesophageal cancer: a multicentre, randomised phase 3 trial. Lancet Oncol. 2014;15:612–9.

20. Li T, Zhao X, Mo Z, Huang W, Yan H, Ling Z, et al. Formononetin promotes cell cycle arrest via downregulation of Akt/Cyclin D1/ CDK4 in human prostate cancer cells. Cell Physiol Biochem. 2014;34:1351–8.

21. Yan X, Shen H, Jiang H, Hu D, Wang J, Wu X. External Qi of Yan Xin Qigong inhibits activation of Akt, Erk1/2 and NF-κB and induces cell cycle arrest and apoptosis in colorectal cancer cells. Cell Physiol Biochem. 2013;31:113–22.

22. Wu X, Yang N, Zhou WH, Xu J, Chen JJ, Zheng FM, et al. Up-regulation of P21 inhibits TRAIL-mediated extrinsic apoptosis, contributing resistance to SAHA in acute myeloid leukemia cells. Cell Physiol Biochem. 2014;34:506–18.

23. Martinez FO, Helming L, Gordon S. Alternative activation of macrophages: an immunologic functional perspective. Annu Rev Immunol. 2009;27:451–83.

24. Lemke G, Rothlin CV. Immunobiology of the TAM receptors. Nat Rev Immunol. 2008;8:327–36.

25. Xiao X, Gaffar I, Guo P, Wiersch J, Fischbach S, Peirish L, et al. M2 macrophages promote beta-cell proliferation by up-regulation of SMAD7. Proc Natl Acad Sci U S A. 2014;111:E1211–20.

26. Franklin RA, Liao W, Sarkar A, Kim MV, Bivona MR, Liu K, et al. The cellular and molecular origin of tumor-associated macrophages. Science. 2014;344:921–5.

27. Xu H, Sun Y, Zhang Y, Wang W, Dan J, Yao J, et al. Protoporphyrin IX induces a necrotic cell death in human THP-1 macrophages through activation of reactive oxygen species/c-Jun N-terminal protein kinase pathway and opening of mitochondrial permeability transition pore. Cell Physiol Biochem. 2014;34:1835–48.

28. Zhang W, Tian J, Hao Q. HMGB1 combining with tumor-associated macrophages enhanced lymphangiogenesis in human epithelial ovarian cancer. Tumour Biol. 2014;35:2175–86.